

## Supporting Information

### *Azephthalocyanine – An Unprecedented Large Twist of a $\pi$ -Conjugation System upon Core-Modification with a Seven-Membered Ring Unit*

Soji Shimizu,\* Hua Zhu, and Nagao Kobayashi\*

*Department of Chemistry, Graduate School of Science, Tohoku University, Sendai 980-8578, Japan*

#### Contents:

- i. Experimental
- ii. HR-ESI-FT-ICR mass spectra
- iii.  $^1\text{H}$  NMR spectra of **4a** and **4b**
- iv. Variable temperature  $^1\text{H}$  NMR spectra of **4a**
- v. Deviation and bond lengths of the selected atoms in **4b**
- vi. Absorption spectra of **3b** and **4b**
- vii. Optimized structures of model compounds of Pc and AZPPcs
- viii. TDDFT calculations
- ix. Cyclic voltammograms
- x. References

#### i. Experimental

**General procedure:** Electronic absorption spectra were recorded with a JASCO V-570 spectrophotometer. Magnetic circular dichroism (MCD) spectra were recorded with a JASCO J-725 spectrodichromometer equipped with a JASCO electromagnet, which produces magnetic fields of up to 1.09 T (1 T = 1 tesla) with both parallel and antiparallel fields. The magnitudes were expressed in terms of molar ellipticity per tesla ( $[\theta]_{\text{M}} / \text{deg dm}^3 \text{ mol}^{-1} \text{ cm}^{-1} \text{ T}^{-1}$ ).  $^1\text{H}$  and  $^1\text{H}$ - $^1\text{H}$  COSY spectra were recorded on a JEOL ECA-600 spectrometer (operating at 594.17 MHz) and a Bruker AVANCE 400 spectrometer (operating at 400.33 MHz) using a residual solvent as an internal reference for  $^1\text{H}$  ( $\delta = 7.26$  ppm for  $\text{CDCl}_3$ ). High resolution mass spectra were recorded on a Bruker Daltonics Apex-III spectrometer. CV and DPV measurements were recorded with a Hokuto Denko HZ5000 potentiostat under nitrogen atmosphere in *o*-dichlorobenzene (*o*-DCB) solutions with 0.1 M of tetrabutylammonium perchlorate (TBAP) as a supporting electrolyte. Measurements were made with a glassy carbon electrode (area = 0.07 cm<sup>2</sup>), an Ag/AgCl reference electrode, and a Pt wire counter electrode. The concentration of the solution was fixed at 0.5 mM and the sweep rates were set to 100 mV/s and 50 mV/s for CV and 10 mV/s for DPV measurements, respectively. The ferrocenium/ferrocene ( $\text{Fc}^+/\text{Fc}$ ) couple was used as an internal standard. Preparative separations were performed by alumina gel column chromatography (Wako), preparative thin layer plate (Silica gel 60, F<sub>254</sub>, Merck), and recycling preparative GPC-HPLC (JAI LC-9201 with preparative JAIGEL-2H, 2.5H, and 3H columns). All reagents and solvents were of commercial reagent grade and were used without further purification except where noted.

**Crystallographic data collection and structure refinement:** Data collection for **4b** was carried out at  $-100$  °C on a Rigaku Saturn CCD spectrometer with graphite monochromatized  $\text{MoK}\alpha$  radiation ( $\lambda = 0.71070$  Å). The structure was solved by a direct method (Sir 2004)<sup>1</sup> and refined using a full-matrix least square technique (SHELXL-97).<sup>2</sup> Yadokari-XG<sup>3</sup> software was used as a GUI for SHELXL-97. CCDC-791481 contains the supplementary crystallographic data for **4b**. These data can be obtained free of charge from the Cambridge Crystallographic Data Centre via [www.ccdc.cam.ac.uk/data\\_request/cif](http://www.ccdc.cam.ac.uk/data_request/cif).

Three toluene molecules are positioned in the unit cell with a slightly disordered fashion and the *tert*-butyl substituents are severely disordered, which is listed as an A level alert after the following refinement. Therefore, these solvent molecules and the substituent parts were refined under thermally and positionally restricted conditions, using DFIX, SIMU, ISOR, DELU, and FLAT commands. Some other large electron densities were observed in the unit cell due to solvent molecules. As we failed to model it properly, the rest molecules were refined without the effect of the unknown solvent molecules by the Platon squeeze technique.<sup>4</sup> There are 813 restraints in the final refinement, of which 72 for DFIX, 12 for FLAT, 99 for DELU, 288 for SIMU, and 342 for ISOR commands.

**Computational methods:** The Gaussian 03 software package<sup>5</sup> was used to carry out DFT and TDDFT calculations using the B3LYP functional with 6-31G(d) basis set. Structural optimization was performed on model compounds of **3a** and **4a** in which the peripheral substituents were replaced with hydrogen atoms for simplicity.

#### General synthetic procedures:

***p*-tert-Butylphenyloxy substituted dibenzoazepiphthalocyanine 4a:** A suspension of 2,2'-biphenyldicarbonitrile<sup>6</sup> (800 mg, 4.00 mmol) and 4,5-di-*p*-tert-butylphenyloxyphthalonitrile<sup>7</sup> (860 mg, 2.00 mmol), ammonium molybdate (800 mg, 4.08 mmol), and anhydrous nickel acetate (140 mg, 0.79 mmol) in 5 ml of dry quinoline was refluxed at 330 °C for 20 min. After removal of the solvent under reduced pressure at 180 °C, the reaction mixture was separated by an alumina column using  $\text{CHCl}_3$  as an eluent to give a green fraction. Preparative thin layer chromatography (TLC, silica gel, 60,  $F_{254}$ , eluent:  $\text{CHCl}_3$ /hexane = 50:1) was employed to remove the remaining byproduct and the blue and green fractions each containing *p*-tert-butylphenyloxy substituted phthalocyanine **3a** and dibenzoazepiphthalocyanine **4a** were collected. The green fraction was further purified by a recycling GPC-HPLC (eluent:  $\text{CHCl}_3$ , detected at 670 nm). The obtained compound was recrystallized from  $\text{CHCl}_3$ /MeOH to afford 4.8 mg of **4a** (0.47%) as a blue solid.

ESI-FT-ICR-MS ( $m/z$ ): 1557.6386 (calcd for  $\text{C}_{98}\text{H}_{92}\text{N}_8\text{O}_6\text{NaNi} = 1557.6391 [M^+ + \text{Na}]$ );  $^1\text{H}$  NMR ( $\text{CDCl}_3$ , 600 MHz, 298 K):  $\delta = 8.55$  (s, 2H;  $\alpha$ -benzo), 8.53 (s, 2H;  $\alpha$ -benzo), 8.37 (s, 2H;  $\alpha$ -benzo), 7.86 (d, 2H; biphenyl,  $J = 7.92$  Hz), 7.58 (dd, 2H; biphenyl,  $J_1 = 8.38$  Hz,  $J_2 = 8.09$  Hz), 7.36 (m, 8H; phenyl), 7.32 (d, 4H; phenyl,  $J = 8.80$  Hz), 7.29 (m, 2H; biphenyl), 7.07 (m, 8H; phenyl), 7.02 (d, 4H; phenyl,  $J = 8.75$  Hz), 6.58 (d, 2H; biphenyl,  $J = 8.31$  Hz), 1.34 (s, 18H; *t*-butyl), 1.33 (s, 18H; *t*-butyl), 1.31 ppm (s, 18H; *t*-butyl); UV/vis ( $\text{CHCl}_3$ ):  $\lambda_{\text{max}}$  [nm] ( $\epsilon$ ) = 353 (41400), 618 (48600), 791 (58300).

***p*-tert-Butylphenyl substituted dibenzoazepiphthalocyanine 4b:** A mixture of 2,2'-biphenyldicarbonitrile (440 mg, 2.20 mmol), 4,5-di-*p*-tert-butylphenylphthalonitrile<sup>8</sup> (440 mg, 1.10 mmol),

ammonium molybdate (400 mg, 2.04 mmol), and anhydrous nickel acetate (85 mg, 0.48 mmol) were added into 3 ml of dry quinoline, and then the suspension was refluxed at 330 °C for 20 min. The solvent was then removed under reduced pressure at 180 °C. The resultant mixture was separated by an alumina column using CHCl<sub>3</sub> as an eluent to remove byproduct. Recycling GPC-HPLC was employed for further purification (detected at 680 nm, CHCl<sub>3</sub>) without purification by TLC. The green fraction was collected and recrystallized from CHCl<sub>3</sub>/MeOH to give 2 mg of **4b** (0.37%) as a dark-blue solid.

ESI-FT-ICR-MS ( $m/z$ ): 1461.6691 (calcd for C<sub>98</sub>H<sub>92</sub>N<sub>8</sub>NaNi = 1461.6696 [ $M^+$ +Na]); <sup>1</sup>H NMR (CDCl<sub>3</sub>, 600 MHz, 298 K):  $\delta$  = 9.06 (s, 2H;  $\alpha$ -benzo), 9.04 (s, 2H;  $\alpha$ -benzo), 8.81 (s, 2H;  $\alpha$ -benzo), 7.91 (d, 2H; biphenyl,  $J$  = 8.09 Hz), 7.60 (dd, 2H; biphenyl,  $J_1$  = 8.23 Hz,  $J_2$  = 8.31 Hz), 7.36 (m, 26H; phenyl (24H) and biphenyl (2H)), 6.68 (d, 2H; biphenyl,  $J$  = 7.87 Hz), 1.37 (s, 18H;  $t$ -butyl), 1.35 (s, 18H;  $t$ -butyl), 1.31 ppm (s, 18H;  $t$ -butyl); UV/vis (CHCl<sub>3</sub>):  $\lambda_{\max}$  [nm] ( $\epsilon$ ) = 357 (35600), 627 (37700), 805 (47100).

## ii. HR-ESI-FT-ICR mass spectra

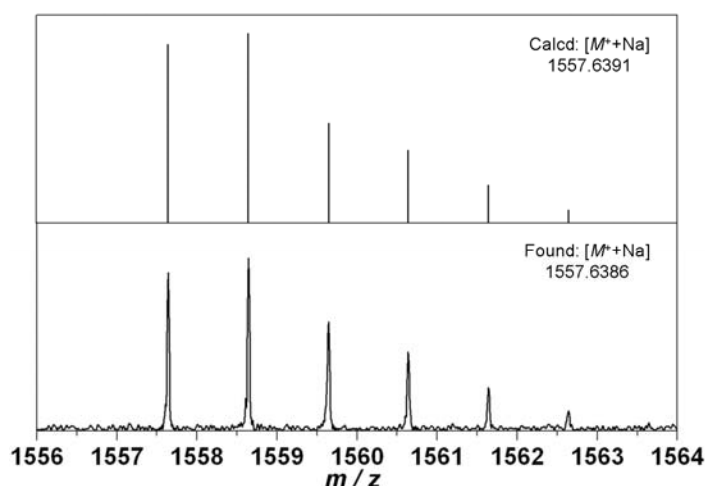


**Figure S1.** Observed high-resolution mass spectrum (bottom) of **4a** and the theoretical isotopic distribution pattern (top).

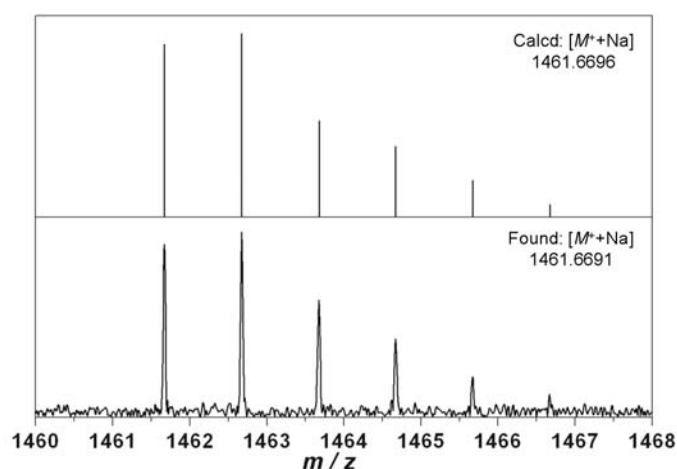


**Figure S2.** Observed high-resolution mass spectrum (bottom) of **4b** and the theoretical isotopic distribution pattern (top).

iii.  $^1\text{H}$  NMR spectra of **4a** and **4b**

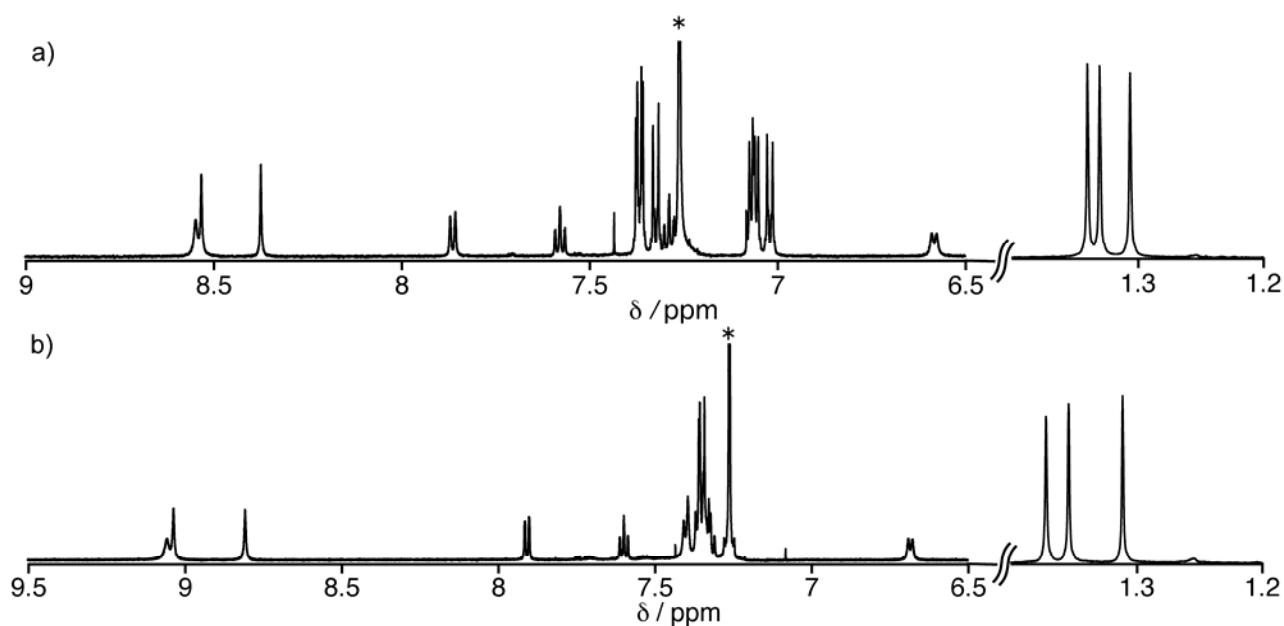


Figure S3.  $^1\text{H}$  NMR spectra of (a) **4a** and (b) **4b** in  $\text{CDCl}_3$  at room temperature. \* indicates a residual solvent peak.

iv. Variable temperature  $^1\text{H}$  NMR spectra of **4a**

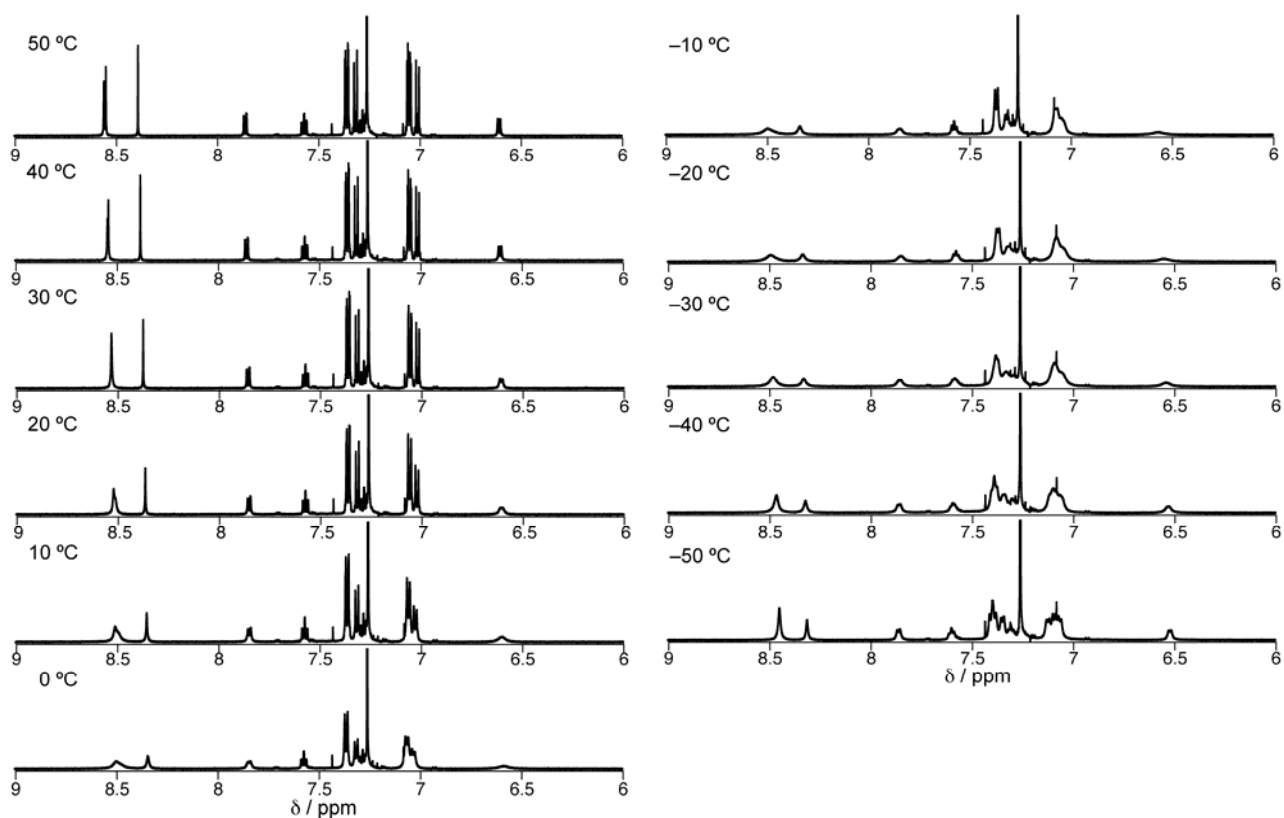
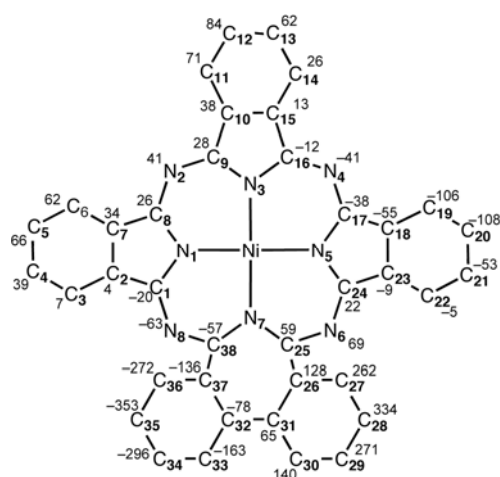


Figure S4.  $^1\text{H}$  NMR spectra of **4a** at variable temperatures in  $\text{CDCl}_3$ . Peaks at 7.26 ppm are due to the residual solvent signals.

v. Deviation and bond lengths of the selected atoms in **4b**



**Figure S5.** Deviation of selected atoms (in 0.01 Å) from the mean plane defined by four coordinating nitrogen atoms (N<sub>1</sub>, N<sub>3</sub>, N<sub>5</sub>, and N<sub>7</sub>).

**Table S1.** Selected bond lengths [Å] in the crystal structure of **4b**.

Ni-N(1)	1.876(3)	Ni-N(3)	1.898(3)
Ni-N(5)	1.874(3)	Ni-N(7)	1.936(3)
N(1)-C(1)	1.356(5)	N(1)-C(8)	1.393(5)
N(2)-C(8)	1.314(5)	N(2)-C(9)	1.329(5)
N(3)-C(9)	1.387(5)	N(3)-C(16)	1.377(5)
N(4)-C(16)	1.341(5)	N(4)-C(17)	1.319(5)
N(5)-C(17)	1.385(4)	N(5)-C(24)	1.363(5)
N(6)-C(24)	1.341(5)	N(6)-C(25)	1.314(5)
N(7)-C(25)	1.366(5)	N(7)-C(38)	1.372(5)
N(8)-C(1)	1.339(5)	N(8)-C(38)	1.318(5)
C(1)-C(2)	1.446(5)	C(2)-C(7)	1.395(6)
C(7)-C(8)	1.447(5)	C(9)-C(10)	1.435(5)
C(10)-C(15)	1.393(5)	C(15)-C(16)	1.450(5)
C(17)-C(18)	1.464(5)	C(18)-C(23)	1.393(5)
C(23)-C(24)	1.435(5)	C(25)-C(26)	1.514(5)
C(26)-C(31)	1.390(6)	C(31)-C(32)	1.462(6)
C(32)-C(37)	1.404(6)	C(37)-C(38)	1.501(5)

vi. Absorption spectra of **3b** and **4b**

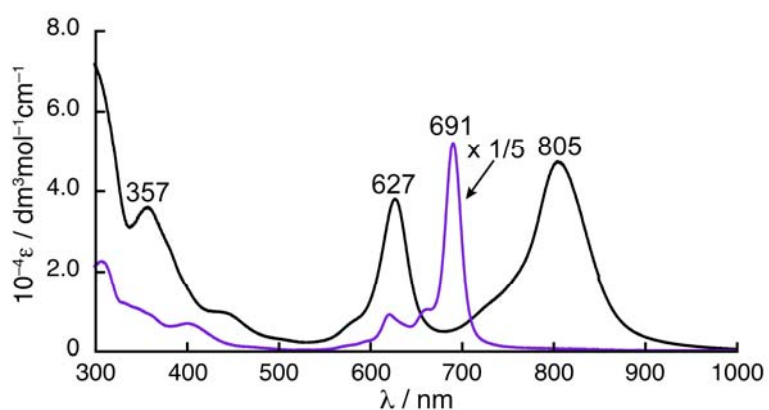


Figure S6. Absorption spectra of **3b** (purple line) and **4b** (black line) in CHCl<sub>3</sub>.

vii. Optimized structures of model compounds of Pc and AZPPCs

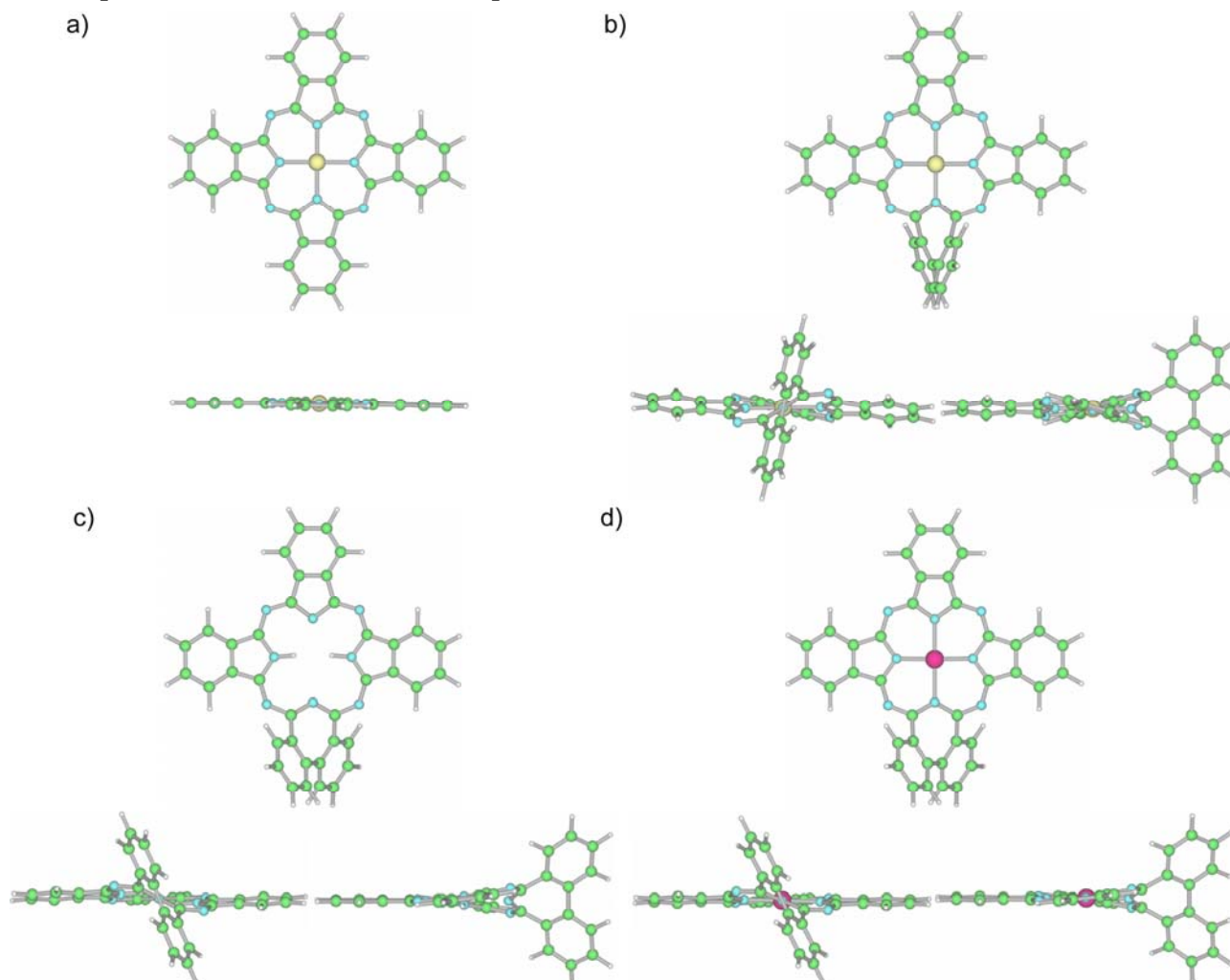


Figure S7. Optimized structures of the model compounds of (a) nickel complex of Pc, (b) nickel complex of AZPPc, (c) free-base of AZPPc, and (d) zinc complex of AZPPc, in which the peripheral substituents were replaced with hydrogen atoms for simplicity; top view (top) and side views (bottom).

### viii. TDDFT calculations

**Table S2.** Selected transition energies and wave functions calculated by the TDDFT (B3LYP/6-31G(d)) method.

compd	energy [nm]	$f^{[a]}$	wave function <sup>[b]</sup>
4a	697	0.33	+ 0.593  167 ← 166> + ...
	593	0.23	+ 0.584  168 ← 166> - 0.113  169 ← 165> + 0.177  169 ← 166> + ...
	341	0.13	+ 0.415  167 ← 160> + 0.215  167 ← 155> - 0.240  167 ← 158> + 0.172  168 ← 163> - 0.324  172 ← 166>
	335	0.16	+ 0.557  167 ← 156> - 0.110  168 ← 159> + 0.124  167 ← 160> - 0.135  167 ← 161> + 0.136  172 ← 166> + 0.204  174 ← 166>
	328	0.15	0.610  174 ← 166> + 0.213  167 ← 155> - 0.149  167 ← 156>
	320	0.17	0.359  168 ← 158> - 0.151  167 ← 152> - 0.170  168 ← 155> + 0.207  168 ← 160> - 0.325  168 ← 161> - 0.321  175 ← 166>

[a] Oscillator strength. [b] The wave functions based on the eigenvectors predicted by TDDFT. Eigenvectors greater than 0.10 are included. The |166> represents the HOMO of **4a**.

### ix. Cyclic voltammograms

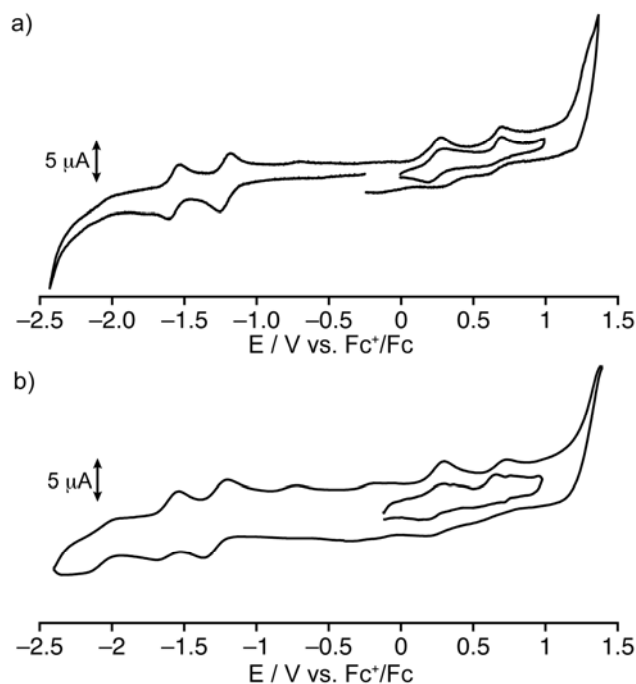


**Figure S8.** Cyclic voltammograms of a) **4a** and b) **4b** in *o*-DCB.

**Table S3.** Redox Potentials of **3a**, **4a**, and **4b** (V vs.  $\text{Fc}^+/\text{Fc}$ ) in *o*-DCB containing 0.1 M TBAP. (Sample concentration = 0.5 mM).  $^a\Delta E_{1/2}^\circ$  is the potential difference between the first oxidation and first reduction potentials.

Compound	Ox <sub>2</sub>	Ox <sub>1</sub>	Red <sub>1</sub>	Red <sub>2</sub>	$\Delta E_{1/2}^\circ$ <sup>a</sup>
<b>3a</b>	---	0.42	-1.39	---	1.81
<b>4a</b>	0.64	0.22	-1.23	-1.59	1.45
<b>4b</b>	0.65	0.25	-1.25	-1.59	1.50

#### x. References

- 1 M. C. Burla, R. Caliendo, M. Camalli, B. Carrozzini, G. L. Cascarano, L. D. Caro, C. Giacovazzo, G. Polidori, and R. Spagna, *J. Appl. Crystallogr.* 2005, **38**, 381.
- 2 G. M. Sheldrick, SHELXL-97, Program for the Solution and Refinement of Crystal Structures, University of Göttingen, Göttingen, Germany, 1997.
- 3 Yadokari-XG, Software for Crystal Structure Analyses, K. Wakita, (2001); Release of Software (Yadokari-XG 2009) for Crystal Structure Analyses, C. Kabuto, S. Akine, T. Nemoto, and E. Kwon, *J. Cryst. Soc. Jpn.*, 2009, **51**, 218.
- 4 (a) A. L. Spek, *Acta Crystallogr., Sect. A* 1990, **46**, c34; (b) P. V. Sluis and A. L. Spek, *Acta Crystallogr., Sect. A* 1990, **46**, 194.
- 5 M. J. Frisch, G. W. Trucks, H. B. Schlegel, G. E. Scuseria, M. A. Robb, J. R. Cheeseman, J. A. Montgomery Jr., T. Vreven, K. N. Kudin, J. C. Burant, J. M. Millam, S. S. Iyengar, J. Tomasi, V. Barone, B. Mennucci, M. Cossi, G. Scalmani, N. Rega, G. A. Petersson, H. Nakatsuji, M. Hada, M. Ehara, K. Toyota, R. Fukuda, J. Hasegawa, M. Ishida, T. Nakajima, Y. Honda, O. Kitao, H. Nakai, M. Klene, X. Li, J. E. Knox, H. P. Hratchian, J. B. Cross, C. Adamo, J. Jaramillo, R. Gomperts, R. E. Stratmann, O. Yazyev, A. J. Austin, R. Cammi, C. Pomelli, J. W. Ochterski, P. Y. Ayala, K. Morokuma, G. A. Voth, P. Salvador, J. J. Dannenberg, V. G. Zakrzewski, S. Dapprich, A. D. Daniels, M. C. Strain, O. Farkas, D. K. Malick, A. D. Rabuck, K. Raghavachari, J. B. Foresman, J. V. Ortiz, Q. Cui, A. G. Baboul, S. Clifford, J. Cioslowski, B. B. Stefanov, G. Liu, A. Liashenko, P. Piskorz, I. Komaromi, R. L. Martin, D. J. Fox, T. Keith, M. A. Al-Laham, C. Y. Peng, A. Nanayakkara, M. Challacombe, P. M. W. Gill, B. Johnson, W. Chen, M. W. Wong, C. Gonzalez, and J. A. Pople, Gaussian 03, Revision E.01, Gaussian, Inc., Wallingford CT, 2004.
- 6 G. Ege and E. Beisiegel, *Synthesis* 1974, 22.
- 7 (a) M. D. Maree and T. Nyokong, *J. Porphyrins Phthalocyanines* 2001, **5**, 555; (b) S. E. Maree and T. Nyokong, *J. Porphyrins Phthalocyanines* 2001, **5**, 782; (c) D. Wöhrle, M. Eskes, K. Shigehara, and A. Yamada, *Synthesis* 1993, 194.
- 8 S. Eu, T. Katoh, T. Umeyama, Y. Matano, and H. Imahori, *Dalton Trans.* 2008, 5476.